

A Nernst heat theorem for nonequilibrium jump processes

Faezeh Khodabandehlou,^{1,*} Christian Maes,¹ and Karel Netočný²

¹*Instituut voor Theoretische Fysica, KU Leuven, Belgium*

²*Institute of Physics of the Czech Academy of Sciences, Prague, Czech Republic*

We generalize a version of the Third Law of Thermodynamics to nonequilibrium processes described as Markov jump dynamics on a finite connected graph. In addition to the stationary heat flux, after a small change in an external parameter, an excess heat flows into the thermal bath at temperature T during relaxation. In contrast with equilibrium, a dynamic condition as well is needed under which that excess heat and the nonequilibrium heat capacity vanish as $T \downarrow 0$: the low-temperature dynamical activity must remain sufficiently high so that relaxation times towards the dominant state do not start to dramatically differ between different initial states.

Keywords: nonequilibrium jump process, excess heat, Nernst heat theorem

I. INTRODUCTION

A standard topic of thermal physics concerns the heat flux between a system and a heat bath as the result of changes in external parameters such as volume or temperature. Regularities emerge when these changes are quasistatic and along equilibria, and then get described by the thermodynamic laws for reversible processes. For example, the Clausius heat theorem identifies a state function, the entropy being the reversible heat by temperature, not ever decreasing for spontaneous processes in a closed and isolated system [1, 2]. That entropy can be measured in terms of heat capacity or from latent heat (when temperature is unchanged), expressing the susceptibility of a system in thermodynamic equilibrium to exchange heat and store energy. As follows from Boltzmann's statistical interpretation of entropy, heat capacities thus yield crucial information about the internal degrees of freedom and their energy distribution of an equilibrium system. To witness, the quantum revolution was much inspired by the difficulty to account in classical physics for

*Electronic address: faezeh.khodabandehlou@kuleuven.be

the low-temperature behavior of specific heats [3]. The Third Law of Thermodynamics, as pioneered by Nernst and Planck, deals explicitly with these questions, [4, 5] where Nernst's version considered the entropy to argue that at zero temperature it becomes a constant independent of any external parameter. Further conditions imply that the heat capacity must vanish with temperature [1, 6]. However, in contrast with the First and Second Law, the Third Law is not always obeyed by substances and corresponding Nernst theorems therefore require nontrivial conditions, [7, 8].

Since longer it has been considered important to develop calorimetry and to find a similar general structure in the study of thermodynamic processes connecting steady states of nonequilibrium systems [9–11]. The point is not at all to formally extend the definition of entropy [12] and there is in fact no pressing need to take thermodynamic limits; rather we wish to obtain quantitative measures of the heat released or absorbed during a quasistatic relaxation to a (new) nonequilibrium condition *because of* (small) changes in control parameters even in small open systems. That need not be restricted to the context of linear irreversible thermodynamics or to close-to-equilibrium processes. Far-from-equilibrium examples within electronics are micro- or nano-scale devices like digital logic circuits with a rich collection of nonlinear dissipative effects due to quantum tunneling, current leakage, etc. [13]. Other examples include driven hopping dynamics on a lattice in contact with a phonon- or photon-bath, where the driving can be electromagnetic or optical. While the driving there can be time-dependent (like when applying an AC-field), here we imagine time-scales where the external field can be taken almost constant. The extension to truly time-dependent external driving is conceptually not different though. Finally, examples of increasing importance arise in life processes [14, 15], where the body or the cell act as thermal reservoir (albeit it not at low temperature) and the driving is mostly chemical. There in particular, reactions occur far from equilibrium and modeling with Markov jump processes becomes very relevant to understand the calorimetry of active systems [16, 17].

In driven systems the heat exchange always runs against a dissipation background. In the stationary situation, work done by nonconservative forces are constantly dissipated as (Joule) heat. Changing an external parameter creates an excess heat in the relaxation to the new steady condition. Then, our interest may go to that excess part coming from changes in the temperature and/or other parameters defining the system dynamics [18–20].

However, how the total heat exchange is split into the “background” and the “excess” is not unique and various schemes exist exhibiting different features. One such a scheme is known as the Hatano-Sasa approach [18], where the total heat is decomposed into the “house-keeping” and the “excess” components in such a way that the excess heat exactly satisfies the (extended) Clausius heat theorem. Other variants of this approach can be found in [19–21]. Yet, the operational accessibility of such an excess heat is not obvious. Another scheme, which goes back to the original proposal by Oono and Paniconi [11], considers the excess heat defined by subtracting the time-integrated steady state heat flux [9], sometimes called the “dynamical component” of heat [22]. While such an excess heat does not satisfy the Clausius relation unless close to equilibrium, it enjoys the important properties of being both “geometrical” (= dependent only on the thermodynamic trajectory) and “reversible” (= antisymmetric with respect to protocol-reversal) in the quasistatic limit. Since it is also operationally accessible (e.g., by an AC-measurement with low-frequency temperature variations), while the steady-state part is sufficiently simple, this becomes a preferential option for the calorimetric analysis of the present paper. Our main result is that for a large and physically motivated class of nonequilibrium systems modeled as Markov jump processes the excess heat vanishes at absolute zero.

As prime example, if the change is provoked by modifying the temperature of the environment, the excess heat (per change in temperature) is rightly called a nonequilibrium heat capacity [23–25]. Under the same conditions, we show it vanishes at zero temperature.

We start with the setup for Markov jump processes on general finite connected graphs, which includes for example active and driven lattice gases. After that comes the exposition of the extended Third Law and the application to heat capacities.

II. SETUP

We consider Markov jump processes on an (arbitrary) finite, simple and connected graph \mathcal{G} . Vertices x, y, z, \dots denote the physical states or conditions on a mesoscopic scale of description, with energy levels $E(x)$ as for instance associated to molecules or lattice gases. The presence of an edge between vertices x, y in the graph signifies the possibility of a transition. Such a Markov dynamics with discrete states can be obtained as the weak-coupling

limit of a (small) quantum system, which is in incoherent contact with one or several heat baths. We remark that the Third law typically breaks down for diffusion processes which are in a way “too classical” (or too coarse-grained).

The transition rate $k(x, y)$ for a jump $x \rightarrow y$ contains kinetic and thermodynamic information summarizing the weak coupling of the system to a thermal bath. The rates are taken to satisfy local detailed balance,

$$\log \frac{k(x, y)}{k(y, x)} = \beta q(x, y) \quad (\text{II.1})$$

where the antisymmetric $q(x, y) = -q(y, x)$ is the heat dissipated in the thermal bath at inverse temperature β ; see [27] and references therein. For example, for a system incoherently coupled to a phonon bath (i.e., in the weak-coupling limit), we have transition rates

$$k(x, x') = \frac{\gamma}{|1 - e^{-\beta q(x, x')}|} \quad (\text{II.2})$$

for $q(x, x') = E(x) - E(x') + W(x, x')$ where $W(x, x')$ is the work done by the external driving. The frequency γ may still depend subexponentially on β but the low-temperature asymptotics is supposed to be given by $\phi(x, x') = \lim_{\beta \rightarrow \infty} \frac{1}{\beta} \log k(x, x')$ where

$$\begin{aligned} \phi(x, x') &= 0 && \text{when } q(x, x') \geq 0 \\ &= q(x, x') && \text{when } q(x, x') < 0 \end{aligned} \quad (\text{II.3})$$

The transition rates may depend on many parameters such as volume or work-functions but we concentrate on the dependence of the rates on temperature (often indicated with a subscript).

An essential quantity in our thermodynamic analysis below is the expected dissipated power or heat flux into the thermal bath, which is

$$\mathcal{P}_\beta(x) = \sum_y k_\beta(x, y) q(x, y) \quad (\text{II.4})$$

when in state x . We always assume there is a unique stationary probability distribution $\rho_\beta^s > 0$ and the stationary dissipated power or heat flux $\langle \mathcal{P}_\beta \rangle_\beta = \sum_x \mathcal{P}_\beta(x) \rho_\beta^s(x) \geq 0$, nonnegative by convexity (II.1), is assumed to be strictly positive to signify the nonequilibrium condition.

III. EXCESS HEAT

We start with an implementation of the excess heat (motivated above) using a quasistatic protocol in parameter space [9, 19, 21, 26], where the global speed of change goes to zero. In

this paper, for simplicity we only work with changes in temperature and keep all the other parameters fixed. More precisely, we consider $\beta(\varepsilon t), t \in [0, \tau/\varepsilon]$, with an image curve Γ . The probability distribution ρ_t^ε solves the time-dependent Master equation

$$\frac{\partial}{\partial t} \rho_t^\varepsilon(x) = \sum_y [k_{\beta(\varepsilon t)}(y, x) \rho_t^\varepsilon(y) - k_{\beta(\varepsilon t)}(x, y) \rho_t^\varepsilon(x)] \quad (\text{III.1})$$

The expected excess heat from the thermal bath at inverse temperature β towards the system is given by

$$Q_\varepsilon := - \int_0^{\tau/\varepsilon} dt \sum_x [\rho_t^\varepsilon(x) - \rho_{\beta(\varepsilon t)}^s(x)] \mathcal{P}_{\beta(\varepsilon t)}(x)$$

and its quasistatic limit can be calculated to yield

$$\lim_{\varepsilon \downarrow 0} Q_\varepsilon = Q(\Gamma) = - \int d\beta \left\langle \frac{dV_\beta}{d\beta} \right\rangle_\beta \quad (\text{III.2})$$

in terms of the quasipotential [23]

$$V_\beta(x) := \int_0^{+\infty} dt [\langle \mathcal{P}_\beta(X_t) | X_0 = x \rangle_\beta - \langle \mathcal{P}_\beta \rangle_\beta] \quad (\text{III.3})$$

Note that (III.2) indeed implements the considered excess heat in the quasistatic limit as “geometric” (invariant under time-reparametrization) and “reversible” (inverting the protocol changes its sign), properties shared with the equilibrium heat. The time-integral in (III.3) converges at all finite temperatures by well-known results on finite-state Markov processes.

We can also write (III.2) as

$$\delta Q = - \langle dV_\beta \rangle_\beta, \quad dV_\beta = d\beta \frac{dV_\beta}{d\beta} \quad (\text{III.4})$$

Since $\langle V_\beta \rangle_\beta = 0$, we have $- \langle dV_\beta \rangle_\beta = \sum_y d\rho_\beta^s(y) V_\beta(y)$ where $d\rho_\beta^s(y)$ is the change of the stationary distribution ρ_β^s under $\beta \rightarrow \beta + d\beta$. In summary and central to our analysis,

$$\delta Q = \sum_y d\rho_\beta^s(y) V_\beta(y) = \langle V_\beta; d \log \rho_\beta^s \rangle_\beta \quad (\text{III.5})$$

where $\langle f; g \rangle = \langle fg \rangle - \langle f \rangle \langle g \rangle$ denotes the stationary covariance, and we used that $\langle d \log \rho_\beta^s \rangle_\beta = 0$. Note that in equilibrium, $V_\beta = E - \langle E \rangle_\beta$ and $\log \rho_\beta^s = -\beta E - \log Z(\beta)$ for the partition function $Z(\beta)$, and thence, the excess heat (= the total heat) gets expressed in terms of the energy-variance. For nonequilibrium, we get two “potentials” (formally, V_β and $\log \rho_\beta^s$) and their structure and mutual correlation shape the excess heat following the response relation (III.5).

IV. THIRD LAW FOR NONEQUILIBRIA

We understand the extended Third Law as the statement that the excess heat (as defined above for quasistatic processes between nonequilibrium conditions) vanishes at absolute zero:

$$\delta Q \rightarrow 0, \quad \text{with } \beta \uparrow \infty \quad (\text{IV.1})$$

The right-hand side in (III.5) depends on the temperature via V_β and via ρ_β^s . In order to show (IV.1), it suffices to show that V_β remains bounded and that $d\rho_\beta^s \rightarrow 0$ for $\beta \uparrow \infty$. As in equilibrium, nonequilibrium extensions of the Nernst heat theorem require conditions.

We start with the static fluctuations encoded in ρ_β^s . We assume there is a unique state x^* so that $\rho_\beta^s(x) \rightarrow \delta_{x,x^*}$ for $\beta \uparrow \infty$, i.e., the stationary distribution becomes concentrated on a single state. Our first condition is somewhat stronger as we require

$$\rho^s(x) = \delta_{x,x^*}(1 + O(\beta^{-2})) \quad (\text{IV.2})$$

as $\beta \uparrow \infty$. That suffices to have $d\rho_\beta^s \rightarrow 0$ for $\beta \uparrow \infty$, and repeats the non-degeneracy condition in equilibrium. To understand its validity we recall the low-temperature asymptotics of static fluctuations. Define

$$\phi^* := \max_z \phi(z), \quad \phi(z) := \max_{\mathcal{T}} \sum_{(x,x') \in \mathcal{T}_z} \phi(x, x') \quad (\text{IV.3})$$

where the maximum is over all spanning trees \mathcal{T} on the graph with \mathcal{T}_z the oriented tree obtained from \mathcal{T} by directing it toward z . The $\phi(z)$ are analogous to the ground state energies in equilibrium, [28–30]. Indeed, from the Kirchhoff formula [31] the stationary distribution has the $\beta \uparrow \infty$ asymptotics,

$$\rho_\beta^s(x) \simeq e^{-\beta[\phi^* - \phi(x)]} \quad (\text{IV.4})$$

We have $\phi^* = \phi(x^*)$. If x^* is the unique maximizer for $\phi(z)$ (in the sense that all other states are suppressed by $O(e^{-\tilde{\varepsilon}\beta})$ for some $\tilde{\varepsilon} > 0$), then the convergence in (A.10) is actually exponentially fast. If there are multiple dominant states (i.e., maximizers), then the convergence $d\rho_\beta^s \rightarrow 0$ may be polynomial in temperature. The dependence of the low-temperature excess heat on the behavior of the stationary condition ρ_β^s is an important instance of

how heat, also in nonequilibrium statistical mechanics, informs about low-temperature degeneracy, extending the connection between Clausius and Boltzmann approaches to entropy.

That the quasipotential V is uniformly bounded at vanishing temperature is mathematically more complicated and, in a general setup, conditions on the transition rates follow from a rigorous application of the matrix-forest theorem as highlighted in Appendix A. As is already clear however from (III.3), boundedness of V strongly relates with low-temperature relaxation properties and in particular with the accessibility of the states that support the zero-temperature condition. In that sense, we need sufficient low-temperature (residual) dynamical activity. The static or even ‘frozen’ picture used to support the 3rd Law for equilibrium systems thus needs to be adapted, and an extra dynamical condition appears for genuine nonequilibrium systems: while relaxing to the dominant state, all initial states should give rise to a comparable amount of energy dissipation in the loops. That is the physics content of the mathematical conditions on the transitions rates given in Appendix A as they imply a “no-delay:” the relaxation times towards the dissipative structure (loops) must be about equal for different initial states.

More precisely, our (second) condition on the transition rates assures that the mutual differences in relaxation times do not exceed the dissipation time scale (= inverse dissipation rate). In the case of a detailed balance dynamics, the dissipation time is infinite and $V_\beta(x) = E(x) - \langle E \rangle_\beta$ is automatically bounded. For an exact mathematical formulation, see Eq. (A.10) in Appendix A.

For more heuristics on the uniform boundedness of $V_\beta = V$ as $\beta \uparrow \infty$, we start with a remark. Consider the edges (xx') in the graph. If the edge differences $|V(x) - V(x')|$ are all bounded, then also the quasipotential V must remain bounded, because, under our conditions, $V(x^*)$ cannot be diverging: the boundedness of the quasipotential over all oriented edges gives the boundedness of the quasipotential in every state.

Putting $f(y) = \mathcal{P}_\beta(y) - \langle \mathcal{P}_\beta \rangle_\beta$, the difference of (III.3) is

$$V(x) - V(x') = \sum_y [G_{xy} - G_{x'y}] f(y) \quad (\text{IV.5})$$

where G_{xy} is the expected residence time in vertex y when starting the process, far in the past, from vertex x . Clearly, if the transitions $x \leftrightarrow x'$ over the edge are not completely damped with $\beta \uparrow \infty$, we may expect a bounded difference $V(x) - V(x')$, as also f is bounded.

The typical time spent for transiting from say x to x' is allowed to grow exponentially with β as long as and to the extent that $f(y)$ cancels that divergence.

Towards a more manageable mathematics, we substitute (II.4) in (III.3), so that we get the equations

$$\sum_{x'} k(x, x') [V(x') - V(x) + q(x, x')] = \langle \mathcal{P}_\beta \rangle_\beta \quad (\text{IV.6})$$

to be satisfied for all states x (while the right-hand side does not depend on x). In the limit $\beta \uparrow \infty$ the transition rates $k(x, x')$ and the dissipated power \mathcal{P}_β remain bounded (while the heat $q(x, x')$ does not depend on temperature). Still, when the rates $k(x, x') \sim \exp(-c\beta)$ for some $c > 0$, get exponentially smaller than the dissipated power $\langle \mathcal{P}_\beta \rangle_\beta$, the differences $|V(x) - V(x')|$ may grow exponentially with β and yet satisfy (IV.6). That is truly the same danger as in the discussion of (IV.5), and is avoided by putting our second condition above.

That can be made mathematically precise as the set of linear equations (IV.6) is actually solvable. The solution is in terms of a graphical representation of the $V(x) - V(x')$; see Appendix A where the mathematics produces an explicit condition on the transition rates. The main step is an application of the matrix-forest theorem, which has tree-loops as the building blocks in the graphical decomposition. In the next example, we take such a tree-loop.

Consider Fig. 1. We suppose frequency $\gamma = 1$ (defining the time-unit) in (II.2) and we take the energy landscape indicated in Fig. 1.

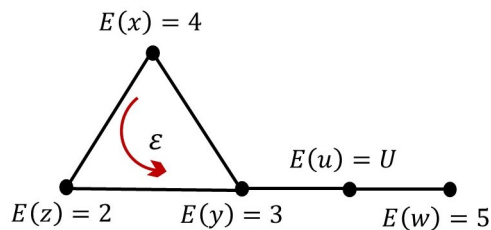


FIG. 1: Example of a tree-loop, building blocks for the solution of (IV.6) following the matrix-forest theorem. As a function of $E(u) = U$ the quasipotential V remains bounded ($U \leq 6$) or not when $\beta \uparrow \infty$.

Additionally, a counter-clockwise constant driving of strength ε is applied around the triangle (loop), but we can take ε arbitrarily small (close-to-equilibrium) to see both the

problem and its solution.

The dissipative structure is the current in the triangle $x \rightarrow z \rightarrow y \rightarrow x$. It is easy to verify that $z = x^*$ (see (IV.4)) is the unique dominant state and that the dissipative power $\langle \mathcal{P}_\beta \rangle_\beta$ is of order $\exp -\beta$, which is the escape rate from z . The energy difference over the outer edge (uw) is $E(w) - E(u) = 5 - U$, which means that $k(w, u) \simeq \exp[-\beta(U - 5)]$ for $U > 5$. Hence, in (IV.6), we can take a bounded edge difference $V(w) - V(u)$ as long as $U \leq 6$. In other words, there is a trap over the edge (w, u) when U is too large, with a too long delay for relaxation for the quasipotential in $V(w)$ to remain bounded. That turns out to be the general scenario.

We summarize the above by repeating that we require (1) a non-degeneracy of the zero-temperature stationary distribution, (IV.4), (2) a non-delay over edges away from the dissipative structure in the relaxation behavior in the excess heat, uniformly in low temperature. That translates in a graphical solution of (IV.6), as mathematically detailed in Appendix A.

V. HEAT CAPACITY

Theory and basic examples of nonequilibrium heat capacities have started with [23, 24]. The heat capacity measures the excess heat *towards* the system per temperature change. The expressions (III.2)–(III.5) allows us, mathematically and physically, to define the heat capacity

$$C(\beta) := \frac{\delta Q}{d\beta^{-1}} = \beta^2 \left\langle \frac{dV_\beta}{d\beta} \right\rangle_\beta \quad (\text{V.1})$$

while we fix the other controls (as for fixed volume specific heats).

As a consequence of the general analysis (and conditions) above, the heat capacity needs to vanish at zero temperature as well, $C(\beta) \rightarrow 0$. The heat capacity goes to zero exponentially fast in $\beta \uparrow \infty$ in the case of a unique dominant state and possibly much slower due to the presence of more than one dominant state. That is how the nonequilibrium heat capacity, similar to its equilibrium counterpart, reveals the support of the zero-temperature distribution.

Breaking the “no-delay” condition discussed around (IV.6), the heat capacity can easily diverge at zero temperature. That may lead to a zero-temperature phase transition, e.g. when the energy barriers between two neighboring nonequilibrium conditions depend on various

thermodynamic and kinetic quantities.

VI. CONCLUSIONS

We have considered nonequilibrium systems described via Markov jump processes on a general finite and connected graph. The excess heat measures the heat given to the system during and entirely due to the relaxation to a nearby nonequilibrium condition. The infinitesimal excess heat is the covariance of the quasipotential V and the change $d \log \rho$ in stationary probability.

Hence, the mathematical strategy for showing a Third Law consists of two steps. First, the low-temperature stationary distribution must have sufficient non-degeneracy. Secondly, a “non-delay”-condition on the rates suffices for V to be uniformly bounded as the temperature reaches absolute zero. Together they imply that the nonequilibrium excess heat vanishes at absolute zero. As a corollary, the nonequilibrium heat capacity vanishes as well with temperature at a rate which depends on the asymptotic structure of the stationary probabilities.

For the physics interpretation of that extended Nernst heat theorem, the “non-delay” condition is an extra dynamical requirement, reflecting the zero-temperature accessibility of the main dissipative structure. That is new with respect to equilibrium.

We have chosen a notion of excess heat which is measurable as the geometric reversible part of the heat. Measuring nonequilibrium heat capacities is a newer challenge though, [32–37]. As explained in [16, 25], an AC-calorimetric scheme should work perfectly well and we hope the present work motivates further experimental work on low-temperature calorimetry for out-of-equilibrium systems.

Appendix A: Mathematical ingredients

We collect here mathematical ingredients, essential for the derivation of the nonequilibrium Nernst heat theorem. More mathematical details make the subject of a separate paper [38]. For an introduction to graphical methods for nonequilibrium purposes, see [29].

We start with graph-theoretical definitions.

A *spanning subgraph* of \mathcal{G} is a graph including all vertices of \mathcal{G} . A *tree* is a connected subgraph without loops. A *spanning tree* is often denoted by \mathcal{T} . A *rooted tree* is an oriented tree having all its edges toward a given vertex called root; \mathcal{T}_x is a spanning tree with root x . A *tree-loop* is made by one loop L to which trees are joined ending at a vertex on the loop. A spanning tree-loop is denoted by H ; see Fig. 2.

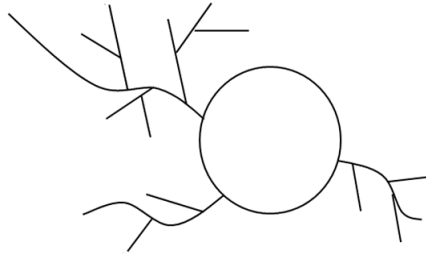


FIG. 2: A tree-loop. Any number of trees may be connected to the loop.

An *oriented tree-loop* is a tree-loop such that all edges have an orientation: the trees are rooted on the loop and the edges on the loop are all oriented clockwise or all counter-clockwise. See Fig.3

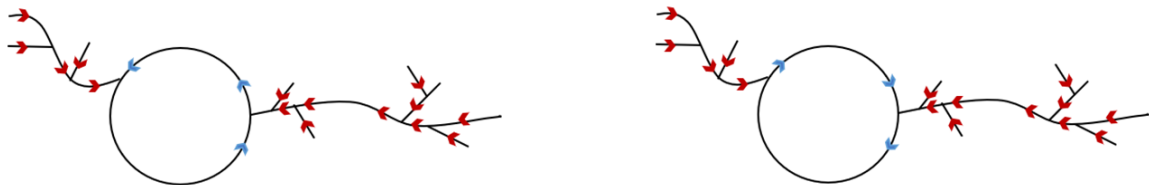


FIG. 3: Oriented tree-loop. The trees are rooted on the loop and the loop can be in two different directions.

A *tree-loop-tree* is a graph including a tree-loop and a separated tree. An oriented *tree-loop-tree* is made by an oriented tree-loop and a rooted tree. Here our meaning of an (oriented) tree-loop-tree is a spanning (oriented) tree-loop-tree. See Fig. 4.

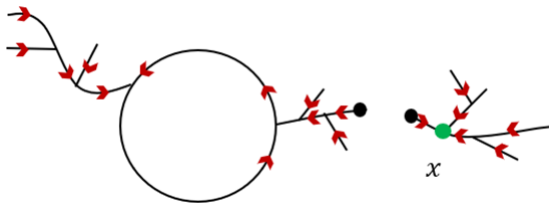


FIG. 4: An oriented tree-loop-tree when the loop is counter-clockwise and the separated tree is rooted on x .

Consider a tree-loop H which includes a certain edge e in the tree-part. If we remove that edge e , then a tree-loop-tree is obtained; see Fig. 5. That tree-loop-tree is denoted by $H^{(e)}$.

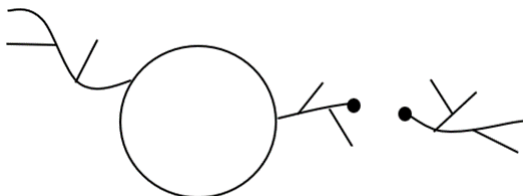


FIG. 5: A tree-loop-tree is made by removing one edge from a tree-loop.

For every $H^{(e)}$ there are different possible orientations (the tree-loop part has two possible directions of the loop and the tree part has different possible roots). The set of all possible orientations of $H^{(e)}$ is denoted by $O(H^{(e)})$.

Oriented graphs obtain their weights as the product of transition rates along all edges. We consider the Markov jump processes of the paper. There is a Kirchhoff formula for the stationary distribution ρ^s ; see e.g. [29, 30] for physical interpretations as well:

$$\rho^s(x) = \frac{w(x)}{W}, \quad w(x) = \sum_{\mathcal{T}} w(\mathcal{T}_x), \quad w(\mathcal{T}_x) = \prod_{(y,y') \in \mathcal{T}_x} k(y, y') \quad (\text{A.1})$$

for normalization $W = \sum_x \sum_{\mathcal{T}_x} w(\mathcal{T}_x)$, and where \mathcal{T}_x is a spanning tree oriented towards vertex x . Such a tree-representation can be extended to give a graphical representation of the quasipotential V_β defined in Eq. III.3.

1. Graphical representation of quasipotential

To show the uniform boundedness of the quasipotential $V = V_\beta$ in $\beta \uparrow \infty$ we use a graphical representation. The difference of the quasipotential over an edge splits in two parts, one related to spanning trees and another related to tree-loops in the underling graph. The notations will be further clarified in an example.

Fix an oriented edge $\bar{e} := (x, x')$ and write $V(\bar{e}) := V(x) - V(x')$. Then,

$$V(\bar{e}) = V_{\text{tree}}(\bar{e}) + V_{\text{loop}}(\bar{e}) \quad (\text{A.2})$$

where the first term contains the weights of rooted spanning trees,

$$V_{\text{tree}}(\bar{e}) = \frac{1}{W} \sum_z \sum_{\mathcal{T}} w(\mathcal{T}_z) q_{\mathcal{T}}(x \rightarrow x'), \quad (\text{A.3})$$

and $q_{\mathcal{T}}(x \rightarrow x')$ sums all $q(z, z')$ with (z, z') located on the path connecting x to x' on the tree \mathcal{T} . The second term is

$$V_{\text{loop}}(\bar{e}) = \frac{1}{W} \sum_{H \in \mathcal{H}_e} \sum_{\bar{H} \in O(H^{(e)})} \sigma_H(\bar{e}) q(\ell_{\bar{H}}) w(\bar{H}) \quad (\text{A.4})$$

where \mathcal{H}_e is the set of all tree-loops H having the edge e in a tree. $H^{(e)}$ denotes a tree-loop-tree created by removing the edge e from the tree-loop H . $O(H^{(e)})$ is the set of all oriented tree-loop-trees giving all possible directions to $H^{(e)}$ and \bar{H} denotes an element of the set $O(H^{(e)})$. (Remember that an oriented tree-loop-tree is a loop with two possible directions clockwise and counter-clockwise and trees connected to the loop must be toward the loop. The separated tree is a rooted tree and all states in this tree are allowed to be a root). $\ell_{\bar{H}}$ is the oriented loop in \bar{H} and $q(\ell_{\bar{H}}) = \sum_{(z, z') \in \ell_{\bar{H}}} q(z, z')$. Finally, $\sigma_H(\bar{e}) = +1$ if the edge \bar{e} is leaving the loop and otherwise, $\sigma_H(\bar{e}) = -1$. Note that if $\mathcal{H}_e = \emptyset$, then $V(\bar{e}) = 0$. Under detailed balance, (A.4) is identically zero.

Example

Consider the graph of Fig. 6.

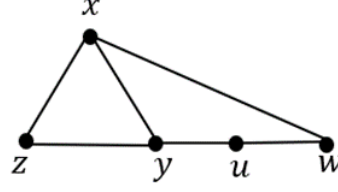


FIG. 6: Example to illustrate the notation.

Denote

$$e_1 := \{x, w\}, e_2 := \{w, u\}, e_3 := \{u, y\}, e_4 := \{y, z\}, e_5 := \{z, x\}, e_6 := \{x, y\}.$$

The graph has six spanning tree-loops, shown in Fig. 7.

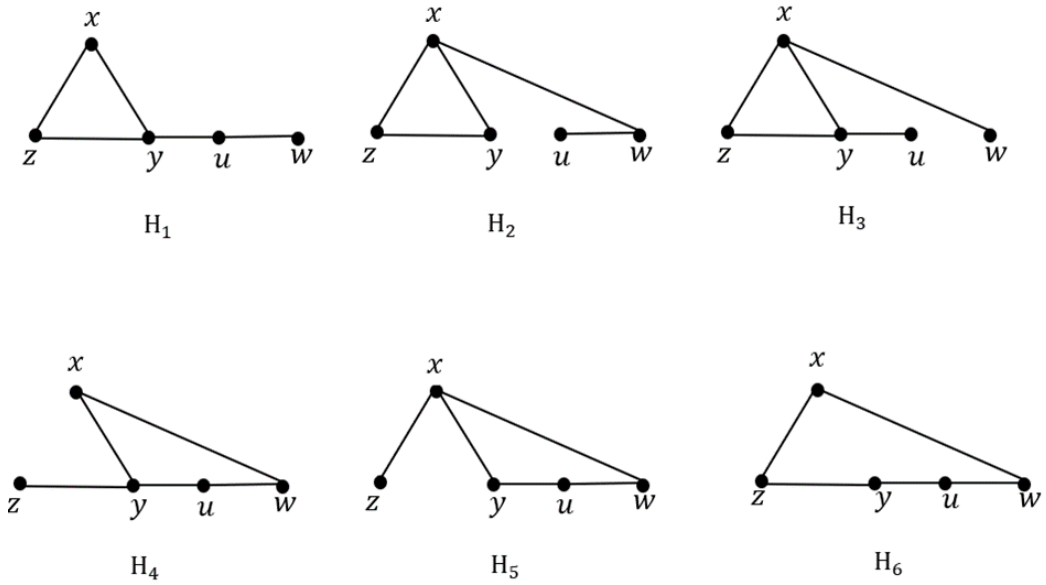
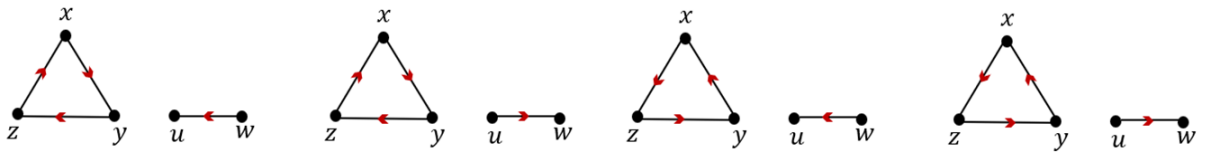


FIG. 7: All tree-loops of the graph in Fig. 6

For every edge a set of spanning tree-loops exists such that all components include the edge on the tree,

$$\mathcal{H}_{e_1} = \{H_2, H_3\}, \mathcal{H}_{e_2} = \{H_1, H_2\}, \mathcal{H}_{e_3} = \{H_1, H_3\}, \mathcal{H}_{e_4} = \{H_4\}, \mathcal{H}_{e_5} = \{H_5\}, \mathcal{H}_{e_6} = \emptyset.$$

In Fig. 8 we show the set $O(H_1^{(e_3)})$ created by removing the edge e_3 from the tree-loop H_1 .

FIG. 8: The components of the set $O(H_1^{(e_3)})$.

Here we can write

$$V_{\text{loop}}(\bar{e}_3) = \frac{1}{W} \left(\sum_{\bar{H} \in O(H_1^{(e_3)})} \sigma_H(\bar{e}_3) q(\ell_{\bar{H}}) w(\bar{H}) + \sum_{\bar{H} \in O(H_3^{(e_3)})} \sigma_H(\bar{e}_3) q(\ell_{\bar{H}}) w(\bar{H}) \right)$$

Proof of (A.2)

We take three steps to show (A.2)–(A.4).

1. For all loops ℓ in the graph \mathcal{G} , and all oriented loops $\bar{\ell}$,

$$\sum_{\bar{e} \in \bar{\ell}} V(\bar{e}) = 0 \tag{A.5}$$

2. The average of $\mathcal{P}(x)$ in (II.4) is (write $\mathcal{P} := \mathcal{P}_\beta$)

$$\langle \mathcal{P} \rangle = \frac{1}{W} \sum_{\bar{H} \in O(\mathcal{H})} w(\bar{H}) q(\bar{\ell}) \tag{A.6}$$

3. For every state (vertex) x ,

$$\sum_{\bar{e}=(x,\cdot)} k(\bar{e}) (-V(\bar{e}) + q(\bar{e})) = \langle \mathcal{P} \rangle \tag{A.7}$$

The proofs of (A.5) and (A.6) are presented in the last section. Here we discuss the proof of (A.7).

To prove (A.7) we are looking at V_{tree} in (A.3) and V_{loop} in (A.4) separately.

Let us start with V_{tree} . Consider the edge $\bar{e} = (x, x')$,

$$\sum_{\bar{e}=(x,\cdot)} k(\bar{e}) V_{\text{tree}}(\bar{e}) = \frac{1}{W} \sum_{\bar{e}=(x,\cdot)} k(\bar{e}) \sum_{z \in \mathcal{V}} \left(\sum_{\mathcal{T} \ni e} w(\mathcal{T}_z) q_{\mathcal{T}}(x \rightarrow x') + \sum_{\mathcal{T} \not\ni e} w(\mathcal{T}_z) q_{\mathcal{T}}(x \rightarrow x') \right) \tag{A.8}$$

If the edge $e = \{x, x'\}$ is located on the spanning tree \mathcal{T} (the first sum), then $q_{\mathcal{T}}(x \rightarrow x') = q(x, x')$. Otherwise $q_{\mathcal{T}}(x \rightarrow z) = (q_{\mathcal{T}}(x \rightarrow x') + q(x', x)) - q(x', x)$, where the two first terms give the sum of q 's over a loop and the third one is $q(x, x')$ which together with the first sum gives $\sum_{\bar{e}=(x,\cdot)} k(\bar{e}) q(\bar{e})$. The rest is

$$\frac{1}{W} \sum_{\bar{e}=(x,\cdot)} k(\bar{e}) \sum_{z \in \mathcal{V}} \sum_{e \notin \mathcal{T}} w(\mathcal{T}_z) (q_{\mathcal{T}}(x \rightarrow x') + q(x', x)) \tag{A.9}$$

The second sum can be split into two cases: when $z = x$ and when the sum is over the states $z \neq x$. Consider the spanning tree \mathcal{T}_x such that $\bar{e} \notin \mathcal{T}_x$. Adding the edge \bar{e} to the tree \mathcal{T}_x makes an oriented spanning tree-loop where the loop is oriented in the same direction with \bar{e} . (Notice that $q_{\mathcal{T}}(x \rightarrow x') + q(x', x)$ is the sum of q 's over the same loop but in the opposite direction.) That shows for the second case that (A.9) is zero. Consider (x, x') to be not on the spanning tree. Then, this edge is located on a loop ℓ_e in the underling graph. It follows that there exist two neighbours of x ; call them x_1 and x_2 . For every z located in the same loop with x, x_1 and x_2 there exist \mathcal{T}_z and \mathcal{T}'_z such that \mathcal{T} and \mathcal{T}' are made by removing the edge $\{x, x_1\}$ and $\{x, x_2\}$ from a spanning tree-loop including loop ℓ_e . Then,

$$k(x, x_1)w(\mathcal{T}_z)(q_{\mathcal{T}}(x \rightarrow x_1) + q(x_1, x)) + k(x, x_2)w(\mathcal{T}'_z)(q_{\mathcal{T}'}(x \rightarrow x_2) + q(x_2, x)) = 0$$

because $(x, x_1) \cup \mathcal{T}_z$ and $(x, x_2) \cup \mathcal{T}'_z$ are the same graphical object. In the case that z is not located on ℓ_e , adding the edge \bar{e} makes an oriented graphical object resembling an oriented spanning tree-loop but one of the trees (including x) is not rooted on the loop. We come back to this point.

Consider $k(\bar{e})V_{\text{loop}}$ and put again $\bar{e} = (x, x')$. The edge \bar{e} is the missing edge in the tree-loop-trees appearing in (A.4). Assume that x is the root of the separated tree and x' is located on the tree-loop part. By adding the edge \bar{e} to the components of the set $O(H^{(e)})$, an oriented spanning tree-loop is made. These oriented spanning tree-loops together with oriented tree-loops remaining from (A.9) yield the sum over all oriented spanning tree-loops. Now consider the case that x is not the root of the separated tree and it is not located on the loop in oriented tree-loop-trees. Take $H \in \mathcal{H}_e$ such that x is not on the loop of H and not the root of the tree part in \bar{H} . Then, x has at least two neighbours, x'_1 and x'_2 . Let $e_1 = \{x, x'_1\}$ and $e_2 = \{x, x'_2\}$, then

$$k(x, x'_1) \sum_{\bar{H} \in O(H^{(e_1)})} \sigma_H(\bar{e}_1)q(\bar{\ell})w(\bar{H}) + k(x, x'_2) \sum_{\bar{H} \in O(H^{(e_2)})} \sigma_H(\bar{e}_2)q(\bar{\ell})w(\bar{H}) = 0$$

because σ_H has different signs. For more than two neighbours on the tree the result is the same. The last case happens when x is located on the loop. Then, adding the missing edge makes a graphical object which is similar to an oriented spanning tree-loop except that one

of the trees is not rooted on the loop and here $\sigma_H = -1$. Finally,

$$\begin{aligned} \sum_{\bar{e}=(x,\cdot)} k(\bar{e}) V(\bar{e}) &= \sum_z k(\bar{e}) (V_{\text{loop}}(\bar{e}) + V_{\text{tree}}(\bar{e})) \\ &= \sum_{\bar{e}=(x,\cdot)} k(\bar{e}) q(\bar{e}) - \frac{1}{W} \sum_H \sum_{\bar{H} \in O(H)} w(\bar{H}) q(\bar{\ell}) \end{aligned}$$

The proof is finished by using (A.6).

2. Boundedness of quasipotential

In this section, we give a proof of the uniform boundedness of the differences of the quasipotential over edges.

Note that $V_{\text{tree}}(\bar{e})$ is uniformly bounded in $\beta \uparrow \infty$ because all weights of spanning trees in the numerator also appear in the denominator, while the coefficient $q_{\mathcal{T}}(x \rightarrow y)$ is bounded as well.

To show the boundedness of $V_{\text{loop}}(\bar{e})$, it therefore suffices to show that $w(\bar{H})/W$ is bounded. Consider an oriented tree-loop-tree $\bar{H} \in O(H^{(e)})$ which is created by removing the edge e from the tree-loop H and then giving direction to the edges. Then, the asymptotic weights are

$$\lim_{\beta \rightarrow \infty} \frac{1}{\beta} \log w(\bar{H}) = \phi(\bar{H})$$

Next, remembering Eq (IV.3) where $\phi^* = \max_y \phi(\mathcal{T}_y)$,

$$\lim_{\beta \rightarrow \infty} \frac{1}{\beta} \log W = \lim_{\beta \rightarrow \infty} \frac{1}{\beta} \log \sum_{\mathcal{T}, y} e^{\beta \phi(\mathcal{T}_y)} = \phi^*$$

Therefore, $V(\bar{e})$ is bounded when (second condition),

$$\text{for all } \bar{H} \in O(H^{(e)}), \phi(\bar{H}) \leq \phi^* \tag{A.10}$$

The following example illustrates how we can check the boundedness of the quasipotential. Consider Fig. 9, as in Fig. 1.

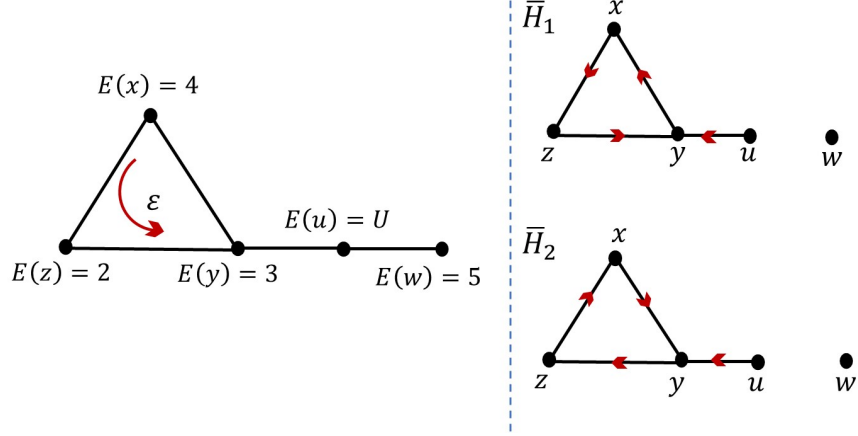


FIG. 9: Example of tree-loop; removing the edge $\{u, w\}$ gives a tree-loop-tree which can have two possible directions (notice that a vertex can be considered as a rooted tree).

We suppose frequency $\gamma = 1$ and the specific energy landscape indicated there and, additionally, a counter-clockwise constant driving of strength $\varepsilon = 1/4$ is applied around the triangle (loop). For energy $E(u) = U \geq 5$, we find $\phi(x, z) = 0, \phi(z, y) = -1 + \varepsilon = -3/4, \phi(y, x) = -1 + \varepsilon = -3/4, \phi(y, u) = 3 - U, \phi(u, w) = 0, \phi(z, x) = -2 - \varepsilon = -9/4, \phi(y, z) = 0, \phi(x, y) = 0, \phi(u, y) = 0, \phi(w, u) = 5 - U$.

We consider two possible values $U = 10$ and $U = 5$, and we focus on the edge $e = (u, w)$ so that $O(H^{(e)}) = \{\bar{H}_1, \bar{H}_2\}$ has two elements shown in Fig. 9. $\phi(\bar{H}_1) = -2 + 2\varepsilon = -3/2, \phi(\bar{H}_2) = -2 - \varepsilon = -9/4$.

In case $U = 10, \phi^* = -5$, and the quasipotential is indeed not bounded.

For $U = 5, \phi^* = 0$ which means that $V(u) - V(w)$ remains bounded for $U = 5$.

Appendix B: Proofs

Here we put the remaining proofs used above for the main results.

Proof of A.5.

Recall the relation (A.2), using the fact that for every three states x, y, x' on a spanning tree $q_{\mathcal{T}}(x \rightarrow y) + q_{\mathcal{T}}(y \rightarrow x') = q_{\mathcal{T}}(x \rightarrow x')$, the sum $\sum_{\bar{e} \in \bar{\ell}} V_{\text{tree}}(\bar{e}) = 0$.

For the loop part, if the underlying graph has only one loop then $H_{\bar{e}} = \emptyset$ for all $\bar{e} \in \bar{\ell}$ and

then $\sum_{\bar{e} \in \bar{\ell}} V_{loop}(\bar{e}) = 0$. We keep our self on the case that there are more than one loop in the graph. Let us take a oriented loop $\bar{\ell}$, we call two of its edges $\bar{e}_1 = (x'', x), \bar{e}_2 = (x, x')$. For the other loop there is a spanning tree-loop $H_{e_1} \not\supset e_2$ such that e_1 is located on a tree and \bar{e}_1 is leaving the loop so that $\sigma_H(\bar{e}_1) = +1$. There is another spanning tree-loop made by removing the edge e_1 from H_{e_1} and adding the edge e_2 , we denote it by $H_{e_2} \not\supset e_1$. The edge \bar{e}_2 in H_{e_2} is oriented towards the loop, then $\sigma_H(\bar{e}_2) = -1$, while $H^{(e_1)} = H^{(e_2)}$. This scenario is repeated for all edges on a loop. Thus it follows $\sum_{\bar{e} \in \bar{\ell}} V_{loop}(\bar{e}) = 0$.

Proof of A.6.

Look at the equation Eq. (II.4) and remember $\langle \mathcal{P} \rangle = \sum_x \mathcal{P}(x) \rho^s(x)$. Applying (A.1),

$$\langle \mathcal{P} \rangle = \frac{1}{W} \sum_y \sum_x \sum_{\mathcal{T}} k(x, y) q(x, y) w(\mathcal{T}_x)$$

Fix the tree \mathcal{T} . If the edge $\{x, y\}$ is in the tree then $k(x, y) q(x, y) w(\mathcal{T}_x) + k(y, x) q(y, x) w(\mathcal{T}_y) = 0$ (the reason is that $(x, y) \cup \mathcal{T}_x$ and $(y, x) \cup \mathcal{T}_y$ are the same graphical objects). We continue with the trees where $\{x, y\} \notin \mathcal{T}$. Consider a spanning rooted tree \mathcal{T}_x (where $(x, y) \notin \mathcal{T}$): there is a path from every state such as y to x . Adding the edge (x, y) to the tree \mathcal{T}_x makes an oriented tree loop such that the loop is oriented in the same direction with the edge (x, y) . For every edge in a loop there is a tree that does not include the edge. We write $\bar{e} = (x_e, y_e)$ and $\bar{e}' = (y_e, x_e)$

$$\begin{aligned} \sum_{x_e} \sum_{y_e} k(\bar{e}) q(\bar{e}) \rho(x_e) &= \frac{1}{W} \sum_{\bar{e}} \sum_{\mathcal{T}} k(\bar{e}) q(\bar{e}) w(\mathcal{T}_{x_e}) \\ &= \sum_{\bar{e}} \sum_{\mathcal{T} \not\supset \bar{e}'} k(\bar{e}) q(\bar{e}) w(\mathcal{T}_{x_e}) = \frac{1}{W} \sum_{\ell} w(\bar{H}_{\ell}) q(\bar{\ell}) = \frac{1}{W} \sum_{\bar{H} \in O(\mathcal{H})} w(\bar{H}) q(\bar{\ell}). \end{aligned}$$

- [1] H. B. Callen, *Thermodynamics and an Introduction to Thermostatistics*. Wiley; 2nd edition (January 16, 1991).
- [2] E. Fermi, *Thermodynamics*. Dover Publications; New Ed edition (June 1, 1956).
- [3] M. J. Klein, Einstein, *Specific Heats and the Early Quantum Theory*. Science, New Series, American Association for the Advancement of Science, vol (148), No. 3667, 173-180 (April 9, 1965).
- [4] W. Nernst, *The New Heat Theorem*. Methuen and Company, Ltd. (1926).

- [5] M. Planck, *Thermodynamik*. 3rd edn (De Gruyter, 1911).
- [6] L. Masanes and J. Oppenheim, *A general derivation and quantification of the third law of thermodynamics*. Nat. Commun. **8**, 14538 (2017).
- [7] E.H. Lieb, *Residual Entropy of Square Ice*. Phys. Rev. **162**, 162 (1967).
- [8] M. Aizenman and E. Lieb, *The third law of thermodynamics and the degeneracy of the ground state for lattice systems*. J. Stat. Phys. **24**, 279–297 (1981).
- [9] T.S. Komatsu, N. Nakagawa, S.I. Sasa and H. Tasaki, *Steady State Thermodynamics for Heat Conduction – Microscopic Derivation*. Phys. Rev. Lett. **100**, 230602 (2008).
—, J. Stat. Phys. **134**, 401 (2009).
- [10] P. Glansdorff, G. Nicolis and I. Prigogine, *The thermodynamic stability theory of non-equilibrium states*. Proc. Nat. Acad. Sci. USA **71**, 197–199 (1974).
- [11] Y. Oono and M. Paniconi, *Steady state thermodynamics*. Prog. Theor. Phys. Suppl. **130**, 29 (1998).
- [12] C. Maes, *Nonequilibrium entropies*. Physica Scripta **86**, 058509 (2012).
- [13] E. Pop, *Energy Dissipation and Transport in Nanoscale Devices*. Nano Res **3**, 147 (2010).
- [14] Eds. Patrick Kent Gallagher, Michael E. Brown and Richard B. Kemp, *Handbook of Thermal Analysis and Calorimetry: From macromolecules to man*, Elsevier, **4**, (1999).
- [15] Ed. Dénes Lörcinzy, *The nature of biological systems as revealed by thermal methods*, Volume 5 of Hot topics in thermal analysis and calorimetry, Springer, (2004).
- [16] P. Dolai, C. Maes and K. Netočný, *Active calorimetry for active systems*. arXiv:2208.01583 (2022).
- [17] F. Khodabandehlou, S. Krekels and I. Maes, *Exact computation of heat capacities for active particles on a graph*. arXiv:2207.11070v1 (2022).
- [18] T. Hatano and S.-I. Sasa, *Steady-state thermodynamics of Langevin systems*. Phys. Rev. Lett. **86**, 3463 (2001).
- [19] C. Maes and K. Netočný, *A nonequilibrium extension of the Clausius heat theorem*. J. Stat. Phys. **54**, 188–203 (2014).
- [20] C. Maes and K. Netočný, *Revisiting the Glansdorff-Prigogine criterion for stability within irreversible thermodynamics*. J. Stat. Phys. **159**, 1286–1299 (2015).
- [21] L. Bertini, D. Gabrielli, D. Jona-Lasinio, and C. Landim, *Clausius inequality and optimality of quasistatic transformations for nonequilibrium stationary states*. Phys. Rev. Lett. **110**, 020601

- (2013).
- [22] Z. Wang, L. Wang, J. Chen, et al. *Geometric heat pump: Controlling thermal transport with time-dependent modulations*. Front. Phys. **17**, 13201 (2022).
 - [23] E. Boksenbojm, C. Maes, K. Netočný, and J. Pešek, *Heat capacity in nonequilibrium steady states*. Europhys. Lett. **96**, 40001 (2011).
 - [24] J. Pešek, E. Boksenbojm, and K. Netočný, *Model study on steady heat capacity in driven stochastic systems*. Cent. Eur. J. Phys. **10**(3), 692–701 (2012).
 - [25] C. Maes and K. Netočný, *Nonequilibrium Calorimetry*. J. Stat. Mech. **114004** (2019).
 - [26] K. Saito and H. Tasaki, *Extended Clausius Relation and Entropy for Nonequilibrium Steady States in Heat Conducting Quantum Systems*. J. Stat. Phys. **145**, 1275-1290 (2011).
 - [27] C. Maes, *Local detailed balance*. SciPost Phys. Lect. Notes **32**, 17pp (2021).
 - [28] C. Maes, K. Netočný and W. O’Kelly de Galway, *Low temperature behavior of nonequilibrium multilevel systems*. Journal of Physics A: Math. Theor. **47**, 035002 (2014).
 - [29] F. Khodabandehlou, C. Maes and K. Netočný, *Trees and forests for nonequilibrium purposes: an introduction to graphical representations*. Journal of Statistical Physics **189**(3), 41 (2022).
 - [30] C. Maes and K. Netočný, *Heat bounds and the blowtorch theorem*. Annales Henri Poincaré **14**(5), 1193–1202 (2013).
 - [31] S. Chaiken and D.J. Kleitman, *Matrix tree theorem*. Journal of combinatorial theory **A24**, 377–381 (1978).
 - [32] J. K. Nielsen and J. C. Dyre, *Fluctuation-dissipation theorem for frequency-dependent specific heat*. Phys. Rev. B **54**, 15754 (1996).
 - [33] M. J. de Oliveira, *Complex heat capacity and entropy production of temperature modulated systems*. arXiv:1905.10306v1 [cond-mat.stat-mech]
 - [34] J. del Cerro and S.Ramos, *Specific heat of latgs ferroelectric crystal under dissipative conditions*. Ferroelectrics Letters, **16**, 119 (1993).
 - [35] H. P. Leiseifer, *Heat Production and Growth Kinetics of E. coli K12 from Flow Calorimetric Measurements on Chemostat Cultures*. Z Naturforsch C J Biosci. **4**, 1036–48 (1989).
 - [36] L. Hansen, R. Criddle, E. H. Battley, *Biological calorimetry and the thermodynamics of the origination and evolution of life*. Pure Appl. Chem. **81**, 1843 (2009).
 - [37] S. Krishnamurthy, S. Ghosh, D. Chatterji, R. Ganapathy and A. K. Sood, *A Micrometer-sized Heat Engine Operating Between Bacterial Reservoirs*. Nature Physics **12**, 1134–1138 (2016).

- [38] F. Khodabandehlou, I. Maes and K. Netočný, *The vanishing of excess heat for nonequilibrium processes reaching zero ambient temperature.* (in preparation).